Journal of Solid State Chemistry **154,** 204–213 (2000)
doi:10.1006/jssc.2000.8837, available online at http://www.idealibrary.com on IDEAL®

Gadolinium and Yttrium Borates: Thermal Behavior and Structural Considerations

M. Th. Cohen-Adad,* O. Aloui-Lebbou,* C. Goutaudier,* G. Panczer,* C. Dujardin,* C. Pedrini,* P. Florian,† D. Massiot,† F. Gerard,‡ and Ch. Kappenstein‡

*LPCML-UMR CNRS 5620, Université Claude Bernard-Lyon I, 43 Bd du 11 Novembre 1918, 69622 Villeurbanne cedex, France; †CNRS-CRPHT, 1D Av. Recherche Scientifique, 45071 Orleans cedex 2, France; and ‡Laboratoire de catalyse en chimie organique, UMR-CNRS 6503, Université de Poitier, 40 Av. du recteur Pineau, 86022 Poitier cedex, France

Received September 9, 1999; in revised form February 10, 2000; accepted February 15, 2000

The present work deals with the phase diagram of the Gd_2O_3–B_2O_3 binary system where three solid phases with respective stoichiometries Gd_3BO_6, $GdBO_3$, and $Gd(BO_2)_3$ have been evidenced. MAS NMR experiments were performed using similar yttrium compounds. Only B^{IV} sites exist in orthoborate at room temperature and the transition phase observed at about 900°C has to be attributed to the change of the boron environment with progressive formation of B^{III} and fast exchange between B^{III} and B^{IV} when temperature increases. MAS NMR results confirm the existence of two yttrium sites. In Y_3BO_6, two threefold and one fourfold boron atoms are observed. One B^{III} corresponds to a planar orthoborate group; the other would be distorted. Fifteen yttrium sites have been observed which are not interpreted yet. © 2000 Academic Press

INTRODUCTION

Many compounds containing rare-earth ions are good candidates for applications in laser and luminescence materials, but the emission is often quenched by doping ion interactions over a critical concentration. The quenching phenomenon is reduced when active ions are separated by large enough anions such as PO_4, WO_4, or BO_3. Particularly, rare-earth borate compounds present a great structural complexity because boron atoms can form planar or nonplanar BO_3 groups, where three oxygen atoms form sp^2 bonds, and also tetrahedral BO_4 groups, where four oxygen atoms form sp^3 bonds (1). Furthermore, borate materials exhibit interesting optical properties due to their high UV transparency and their exceptional optical damage threshold, allowing them to be used in vacuum discharge lamps or screens.

The general objectives of this work concern the luminescence properties of some rare-earth borates doped by Ce^{3+} and Yb^{3+} in relation to the environmental structure of the activator ion, which is influenced by the localized bonding arrangements of the borate groups.

This first paper focuses on the gadolinium borates. It concerns essentially the study of the different solid phases formed in the binary system Gd_2O_3–B_2O_3 and of the structural environments of boron and rare-earth atoms in these compounds.

EXPERIMENTAL PART

$(1-x)Ln_2O_3$–xB_2O_3 samples with Ln = Gd, Y, or Yb were prepared by solid-state reactions. The starting materials were mixtures of Ln_2O_3 and H_3BO_3 powders, to which an excess amount of boric acid (between 5 and 10 mol%) was added in order to compensate for the loss due to the evaporation of B_2O_3 during the firing. After pressing under 4000 kg cm^{-2} to form cylinders of 13 mm of diameter, samples were heated under an air or oxygen (P_{O_2} = 1 bar) atmosphere. Several grinding and firing cycles were needed to obtain complete reaction and well-crystallized specimens.

The nominal composition was calculated through the weight losses during each thermal treatment and controlled by boron and Ln titrations.

Samples were characterized by X-ray diffraction measurements using a Philips PW 3710 diffractometer at Cu$K\alpha$ radiation. The phases were identified by comparison with an X-ray diffraction pattern known for analog compounds or given in the literature.

Thermal behavior of samples was followed by X-ray diffraction and by differential thermal analysis associated to thermogravimetry using a Setaram TAG 24 analyzer working under 1 bar of oxygen. Heating and cooling rates were fixed at 5°C min^{-1}.

MAS NMR experiments were carried out on a Bruker DSX 400 spectrometer operating at principal field of 9.4 T with Larmor frequencies for ^{89}Y and ^{11}B of 19.6 and 128 MHz, respectively. For ^{11}B, the spinning speed was between 12,000 and 13,000 t s^{-1} and for ^{89}Y, it was between 4000 and 5000 t s^{-1}. Chemical shifts have been reported

0022-4596/00 $35.00

relative to B_2O_3 in saturated solution for ^{11}B and to a 1 M solution of $Y(NO_3)_2$ in nitric acid solution for ^{89}Y. The quadrupolar coupling constant C_Q and the quadrupolar asymmetric parameter η_Q have been extracted by simulation using a modified version of the Bruker Winfit program.

Raman spectra were drawn between room temperature and 1200°C using a DILOR XY with an excitatrice wavelengh of 514 nm.

RESULTS

In this work, the phase equilibria in the Gd_2O_3–B_2O_3 binary system has been previously determined as a good tool for preparing pure and well-crystallized materials. For each solid phase observed, the best thermal conditions are given in Table 1.

1. *Phases Equilibria in the Gd_2O_3–B_2O_3 Binary System*

The binary system has been drawn between 20 and 90 mol% $BO_{1.5}$ content and is shown in Fig. 1. Three solid phases, $GdBO_3$, Gd_3BO_6, $Gd(BO_2)_3$, and a demixion liquid–liquid field are observed. The gadolinium orthoborate with formula $GdBO_3$ melts congruently at 1580 ± 20°C, in good agreement with the Levin *et al.* data (2). It takes part into two eutectic reactions:

— the first one at 1575°C corresponds to the reaction liq. $\Leftrightarrow GdBO_3 + Gd_3BO_6$;
— the second one at 1275°C is a monotectic equilibrium liq. $\Leftrightarrow$ liq. + $GdBO_3$.

In the range between 875 and 940°C, orthoborate presents a phase transition with high thermal hysteresis during the cooling. The small difference of the transition temperature between sub- and hyperstoichiometric specimens evidences a very narrow homogeneity field (about 0.2 $BO_{1.5}$ mol%) around the theorical stoichiometry $GdBO_3$.

TABLE 1
Thermal Conditions to Prepare Pure and Well Crystallized Borate Phases Belonging to Gd_2O_3–B_2O_3 Binary System

Compounds	Temperature of the heat treatment (°C)	Time (h)	Observed phases
Gd_3BO_6	400	5	$Gd_3BO_6 + GdBO_3$
	1200	20	
	1300	10	Gd_3BO_6
$GdBO_3$	400	5	$GdBO_3 + Gd(BO_2)_3$
	1100	10	
	1450	1	$GdBO_3$
$Gd(BO_2)_3$	400	5	$Gd(BO_2)_3 + B_2O_3$
	1040	20	
	1040	20	$Gd(BO_2)_3$

At about 1400°C, a probable polymorphic transition leads to a high temperature form which was not indexed but which could be attributed to the formation of a structure type (H)$NdBO_3$ as it was seen for La and Nd orthoborates. Gd_3BO_6 is peritectically decomposed at 1590 ± 20°C into a liquid (about 48 mol% $BO_{1.5}$) and Gd_2O_3, and at 1575 ± 20°C, it participates in an eutectic reaction corresponding to liq. $\Leftrightarrow GdBO_3 + Gd_3BO_6$. The phase $Gd(BO_2)_3$ presents a peritectic decomposition at 1085 ± 20°C given $GdBO_3$ and a liquid rich in B_2O_3 (about 90 mol% of $BO_{1.5}$).

For the three solid phases, the X-ray diffraction patterns at room temperature are given in Fig. 2.

$GdBO_3$ displays hexagonal symmetry and the cell parameters calculated using the space group $P\bar{6}c2$ are $a = 6.62$ Å, $c = 8.80$ Å. For Gd_3BO_6, the main lines have been attributed using the literature data concerning Eu and Tb (3). The proposed space groups are $C2/m$, $C2$, or Cm and the cell parameters calculated from our results and for a monoclinic symmetry are $a = 18.52$ Å, $b = 3.70$ Å, $c = 14.21$ Å, $\alpha = \gamma = 90°$, $\beta = 120.7°$. The structure of the metaborate $Gd(BO_2)_3$ is well known. It crystallizes in the space group $I2/c$ (4). The cell parameters calculated from the diffraction pattern are in good agreement with the literature values: $a = 7.82$ Å, $b = 8.03$ Å, $c = 6.26$ Å, $\alpha = \gamma = 90°$, $\beta = 93.7°$.

2. *Structural Considerations Concerning $GdBO_3$ and Gd_3BO_6*

As the structure of the metaborate $Gd(BO_2)_3$ has been well investigated (4), the structural considerations focused only on the two phases $GdBO_3$ and Gd_3BO_6. The structural modification of $GdBO_3$ at about 900°C has been reinvestigated using X-ray diffraction, Raman spectroscopy, and ^{11}B MAS NMR due to the considerable ambiguity regarding the disposition of boron and the influence of temperature for rare-earth orthoborates between Sm to Lu including Y (5–11).

$GdBO_3$ is not isostructural of vaterite and is referred to as "borate with YBO_3 structure" (5). From X-ray diffraction patterns four structures have been proposed:

1. The first structural determination (6) proposed a hexagonal symmetry with two molecules in the unit cell. The considered space group is $P6_3/mmc$ and it was assumed that the structure of the borate group corresponded to that of a T-shaped monomeric BO_3^{3-} ion.

2. The second structure proposed by R. E. Newnham *et al.* (7) for YBO_3 involved monomeric planar and triangular BO_3^{3-} anions inclined to one another but parallel to the c axis with two possible arrangements, leading a disordered (space group $P6_3/mmc$) or an ordered (space group $P6_3/mcm$) hexagonal structure. In these structures, each

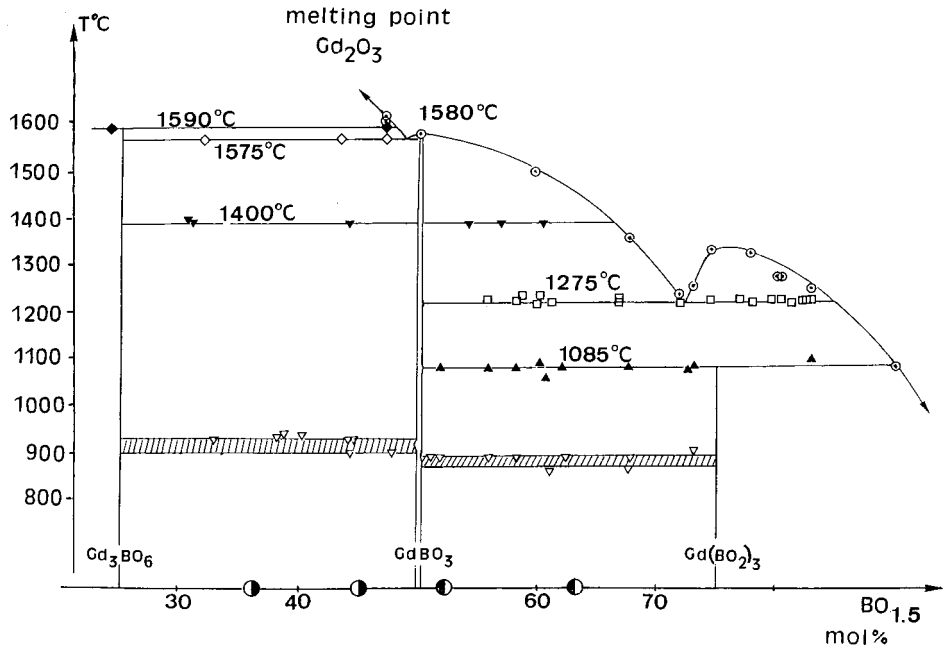

FIG. 1. Phase equilibria in the Gd_2O_3–B_2O_3 binary system.

rare-earth ion would be coordinated to a distorted cube with eight oxygen atoms.

3. Infrared absorption analysis (5, 8–10) disclosed that boron would be in fourfold coordination with a cyclic trimeric structure. Two models were proposed for $YbBO_3$ and are consistent with the optical and absorption properties and with the X-ray diffraction powder patterns. They involve edge-sharing nets of YbO_6 octahedra decrypting polyhedra where a 12-coordinated Yb is in special position surrounded by borate groups and lead

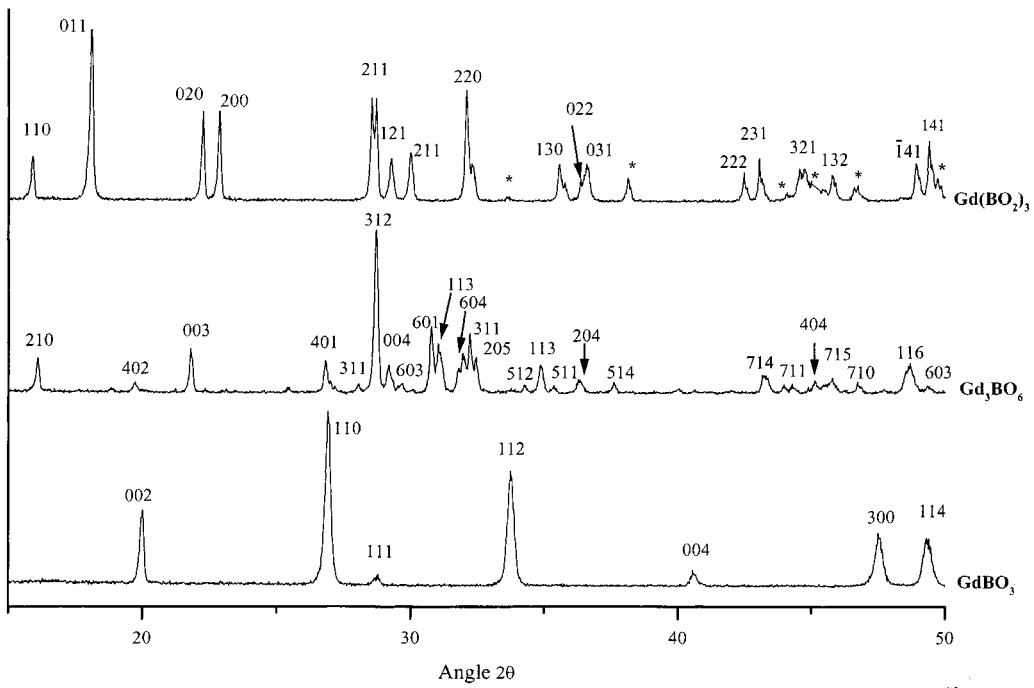

FIG. 2. X-ray diffraction patterns of the different solid phases observed in the Gd_2O_3–B_2O_3 binary system. *, Main lines corresponding to B_2O_3.

to a low- and a high-temperature form. The low-temperature form had the probable space group $P\bar{6}c2$, where the strict requirements of the optical and absorption spectra criteria make it necessary to choose tetrahedral borate groups. The high-temperature form had the probable space group $P6_322$, where boron and oxygen ions are to be accomodated as borate triangles inclined to the c axis (11).

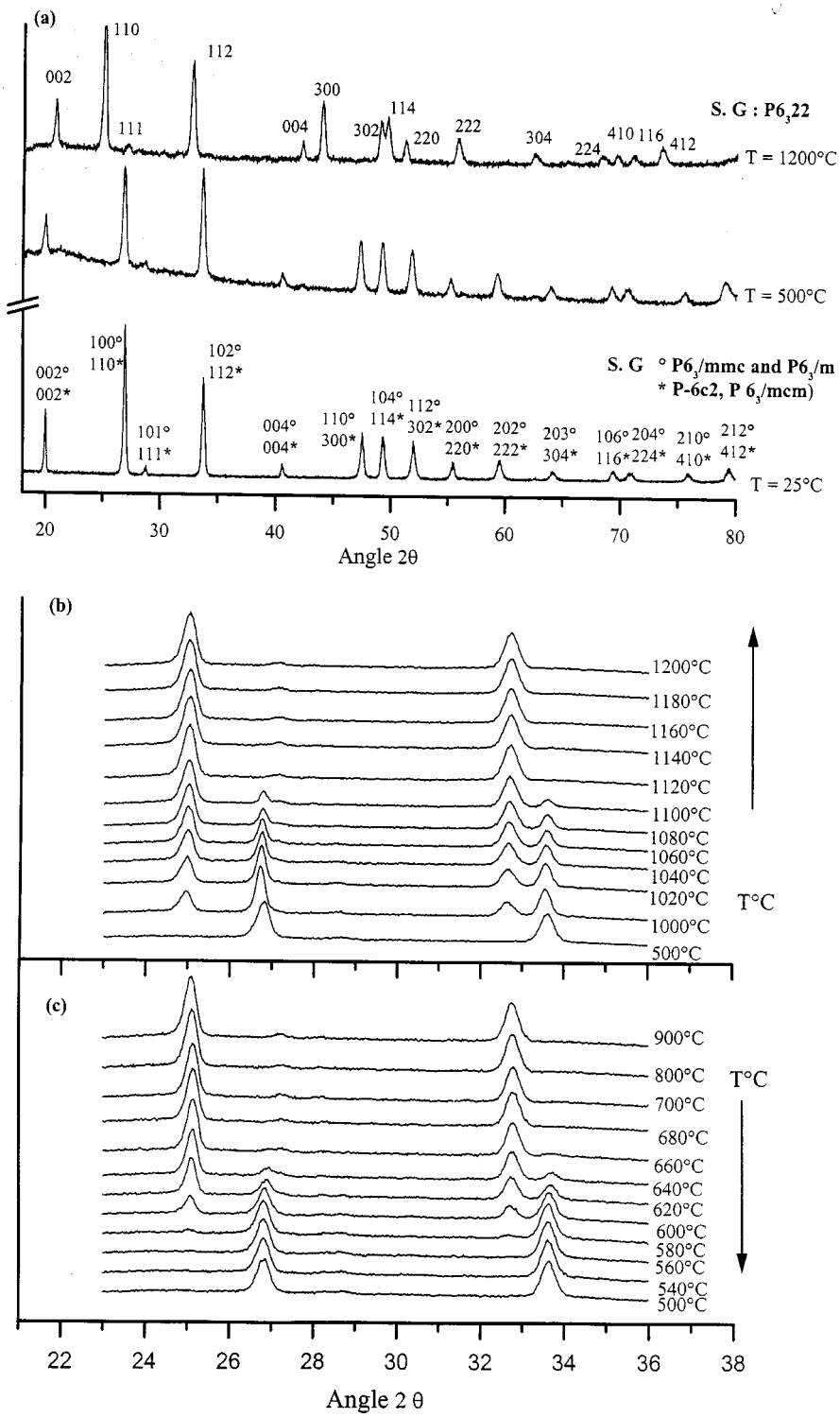

FIG. 3. X-ray diffraction patterns of $GdBO_3$. (a) Low- and high-temperature forms; (b) progressive change with increase of temperature; (c) large hysteresis when sample is cooled from high temperature.

TABLE 2
Temperature Range of the Structural Modification in Dependence on Nature of the Rare Earth Ion

Nature of the ion	Ionic radii (Å)	Beginning of thermal peak (°C)	End of thermal peak (°C)
Gd^{3+}	0.938	882	910
Y^{3+}	0.900	940	971
Yb^{3+}	0.868	988	1009

4. Recently, a new structure was proposed for YBO_3 (12). It would be solved in the $P6_3/m$ space group and yttrium atoms would be eightfold coordinated by oxygen atoms in a trigonal bicapped antiprisms forming a $[YO_8]$ framework. The yttrium atoms would present a unique coordination but two different environments due to a statistical distribution of two oxygen atoms with a partial occupancy (1/3).

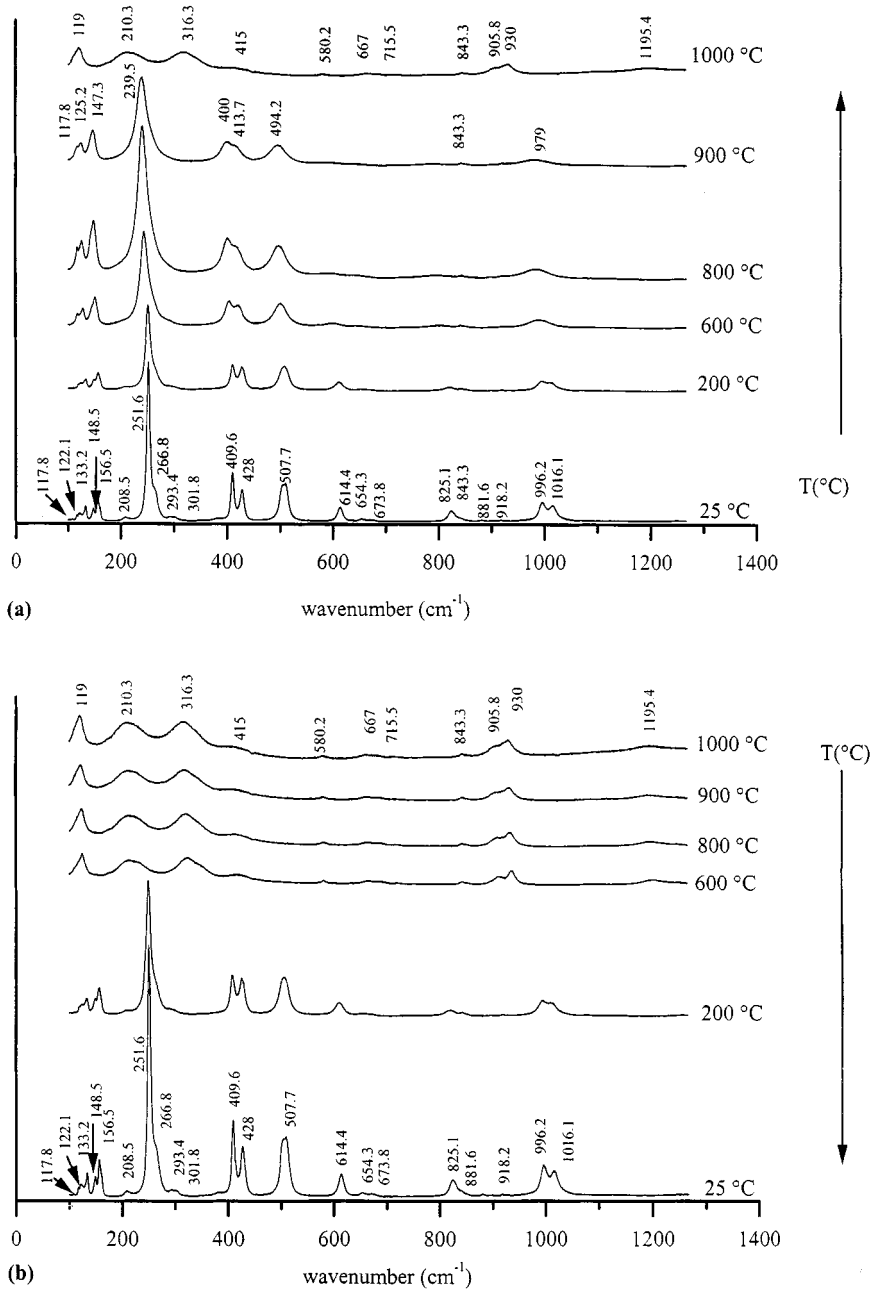

FIG. 4. Raman spectra of $GdBO_3$. (a) At room temperature and when temperature increases; (b) large hysteresis when sample is cooled from high temperature.

TABLE 3
Vibrational Assignment Based on Denning and Ross's Work (5)

Wavenumber (cm^{-1})	Assignment
1016.1	Terminal stretching $\nu_{10}(E')$ or ring stretching $\nu_9(E')$
996.2	Terminal stretching $\nu_{10}(E')$ or $\nu_2(A_1')$ or ring stretching $\nu_8(E')$
917.5	Terminal stretching $\nu_5(A_2'')$ or ring stretching $\nu_8(E')$
825.1	Ring stretching $\nu_9(E')$ or $\nu_8(E')$ and/or terminal stretching $\nu_2(A_1')$ or $\nu_{14}(E'')$
614.4[a]	Ring stretching $\nu_1(A_1')$
507.7[a]	Ring bending $\nu_4(A_1')$
428	Terminal bending $\nu_{11}(E')$ or $\nu_{12}(E')$
409.6[a]	Ring bending $\nu_{13}(E')$
301.2[a]–293.4[a]	Terminal bending $\nu_{16}(E')$
251.7[a]	Terminal bending $\nu_{12}(E')$ and $\nu_3(A_1')$

[a]Assumptions providing the framework on which were built the assignments presented in the Denning and Ross work.

From our X-ray diffraction measurements it has been shown that:

— At low temperature, the powder pattern is consistent with those of the $P6_3/mmc$, $P\bar{6}c2$, $P6_3/mcm$, and $P6_3/m$ space groups (Fig. 3a); the difference concerns the assignment of the lines and some very very weak lines which are better accounted for the $P\bar{6}c2$ space group.

— At high temperature, the X-ray diffraction diagram is consistent with $P6_322$ (Fig. 3a).

— The transition observed at about 900°C is associated with a progressive and slow space group change which occurs over a large range of temperatures and with a large hysteresis when the sample is cooled (Figs. 3b and 3c). The comparison between Figs. 3b and 3c shows the reversibility of the structural transition.

The low- to high-temperature transition involves expansion along the *a* axis and shrinkage in the *c* direction. The cell parameters have been calculated using the space group

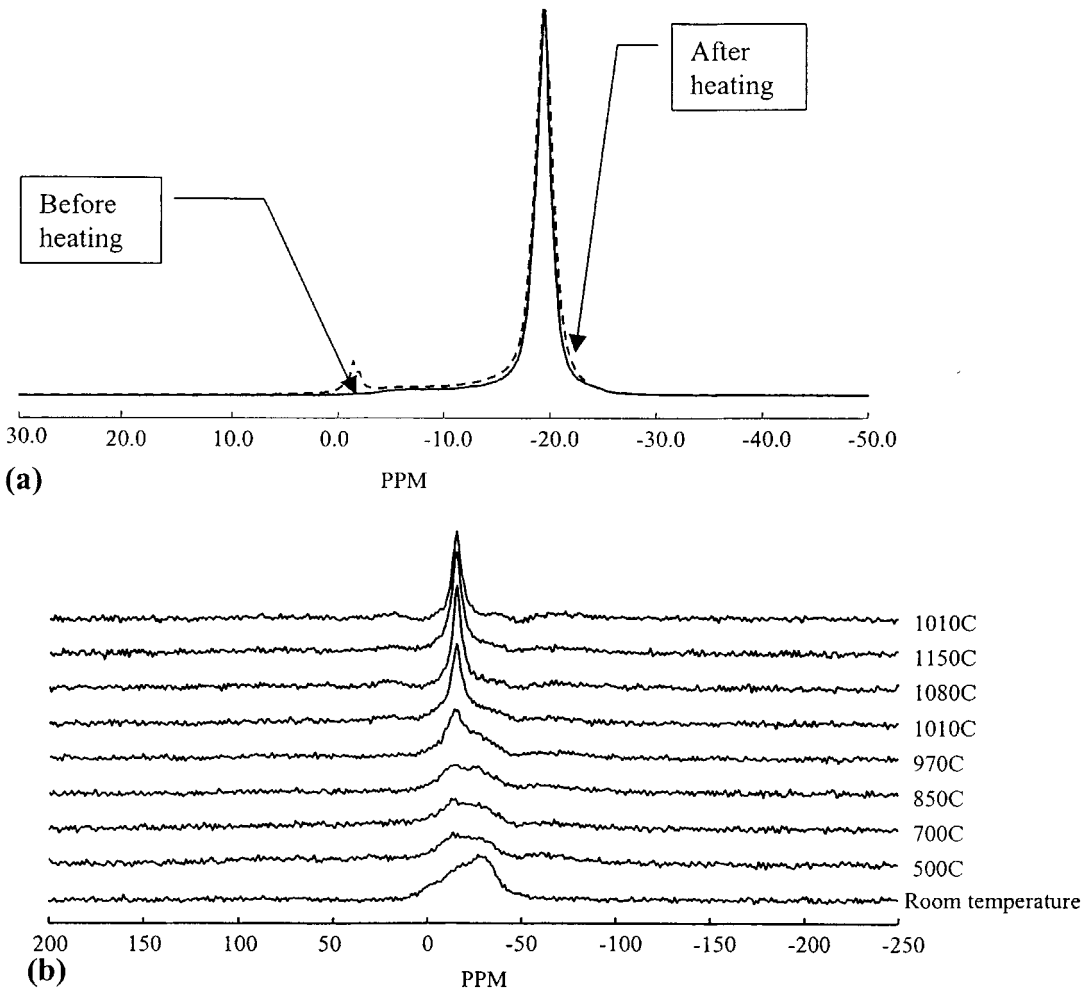

FIG. 5. ^{11}B spectra at 9.4 T of YBO_3. (a) At room temperature before and after heating; (b) high static ^{11}B NMR experiments when temperature increases.

$P\bar{6}c2$, and the values are

$a = 6.64$ Å $\quad c = 8.88$ Å $\quad$ at 500°C

$a = 7.12$ Å $\quad c = 8.55$ Å $\quad$ at 1200°C.

Similar progressive transition occurs (Table 2) when Gd is substituted by Y or Yb and for $YbBO_3$, the temperature range where the low–high transition is observed is in good agreement with the literature data (13).

The Raman spectrum of $GdBO_3$ at room temperature is given in Fig. 4a and agrees with the only one proposed in the literature (5). About 25 bands are observed between 1250 and 100 cm^{-1}. Involving a planar ring with D_{3h} symmetry, a possible assignment of the strongest bands may be proposed (5); it is given in Table 3. There is no absorption above 1016.1 cm^{-1} as is expected for borate not having boron in threefold coordination with oxygen atoms.

Up to 900°C, the main modifications concern the following (Fig. 4a):

— the progressive decrease of the group between 1016.1 and 614.4 cm^{-1} (most of these bands disappear, except those located at 1016.1 and 996.2, which are modified into a unique band at 979 cm^{-1}, and those at 843.3 cm^{-1}, which remain up to 1000°C);

— a small shift of the bands toward the left for the major part of the bands.

The group between 507.7 and 100 cm^{-1} is present up to 900°C, except for the small vibrations at 266.8, 293.4, and 301.8, which disappear when temperature increases.

Between 900 and 1000°C, the Raman spectrum drastically changes and a weak band appears at 1195.4 cm^{-1}, where it may be expected if triangularly coordinated boron atoms are formed.

The change of the atomic arrangement in borate groups induces a structural transition. Figure 4b shows the return toward the initial state when sample is cooled, proving the reversibility of the transformation.

Due to the magnetic properties of gadolinium, the boron and rare-earth environments were investigated by MAS NMR using YBO_3 as a good representative compound.

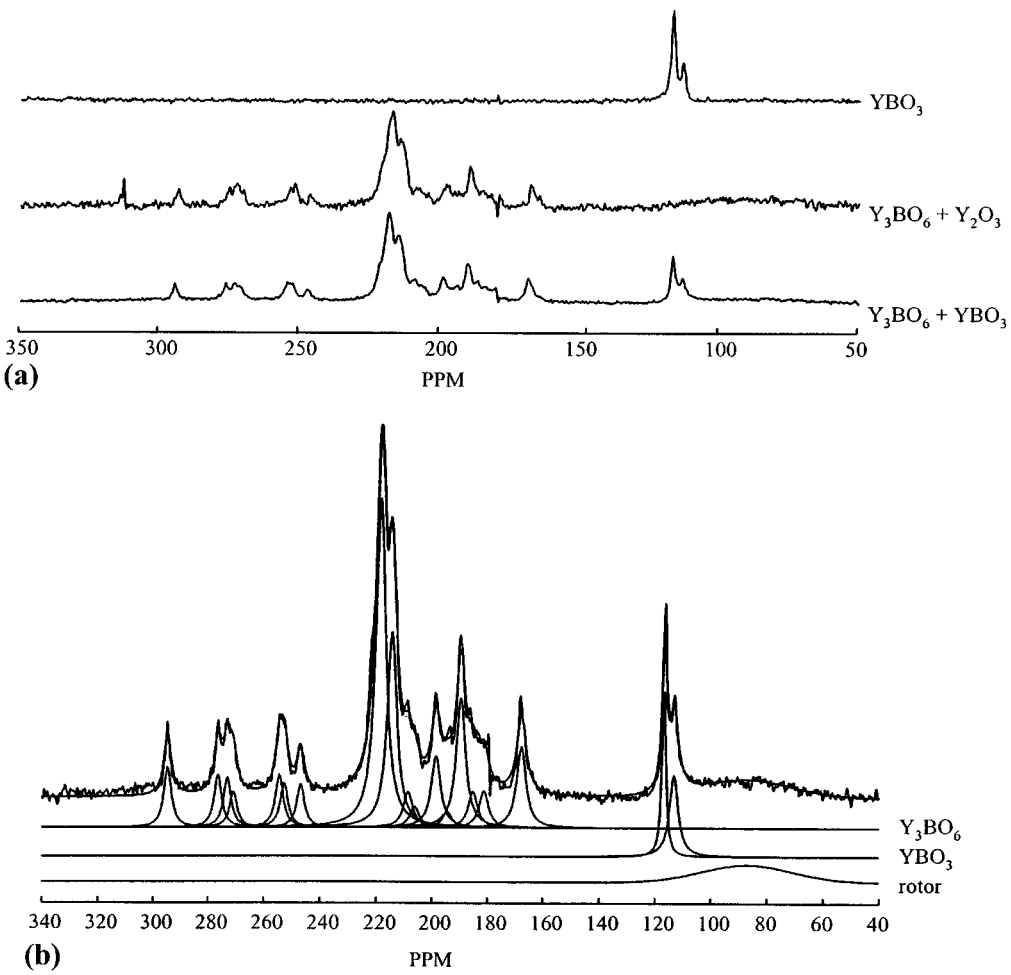

FIG. 6. ^{89} Y spectra at 9.4 T of YBO_3 and Y_3BO_6. (a) Experimental spectra; (b) details of the simulation.

^{11}B. At room temperature, an unique fourfold coordinated boron site (Fig. 5a) is observed with a chemical shift $\delta_{iso} = -20$ ppm. This result is confirmed by the simulation of the experimental curve. Very high static ^{11}B NMR experiments clearly show the existence of a narrow signal above 970°C and a continuous shift of the line to the left (Fig. 5b) when temperature increases. After cooling (Fig. 5a), the ^{11}B MAS NMR line returns to its initial position. A residual line located at 0 ppm can be attributed to condensed free B_2O_3 formed during the heating. This unusual behavior suggests that the structural modification with temperature could be attributed to a sudden increase of the boron mobility. At high temperature, the chemical shift δ_{iso} at about 14 ppm is in the range between B^{IV} and B^{III} and could traduce a progressive formation of B^{III} with a fast exchange between B^{III} and residual B^{IV}. This result argues for the Bradley *et al.* (11) structural proposition but disagrees with the Chadeyron *et al.* data (12).

^{89}Y. Spectra obtained by ^{89}Y MAS NMR are shown in Fig. 6. Two sites are clearly distinguished by simulation. From the results of simulation, if three rare-earth atoms are considered, one is located on a different site. This result agrees with the structure proposed by Bradley *et al.* (11).

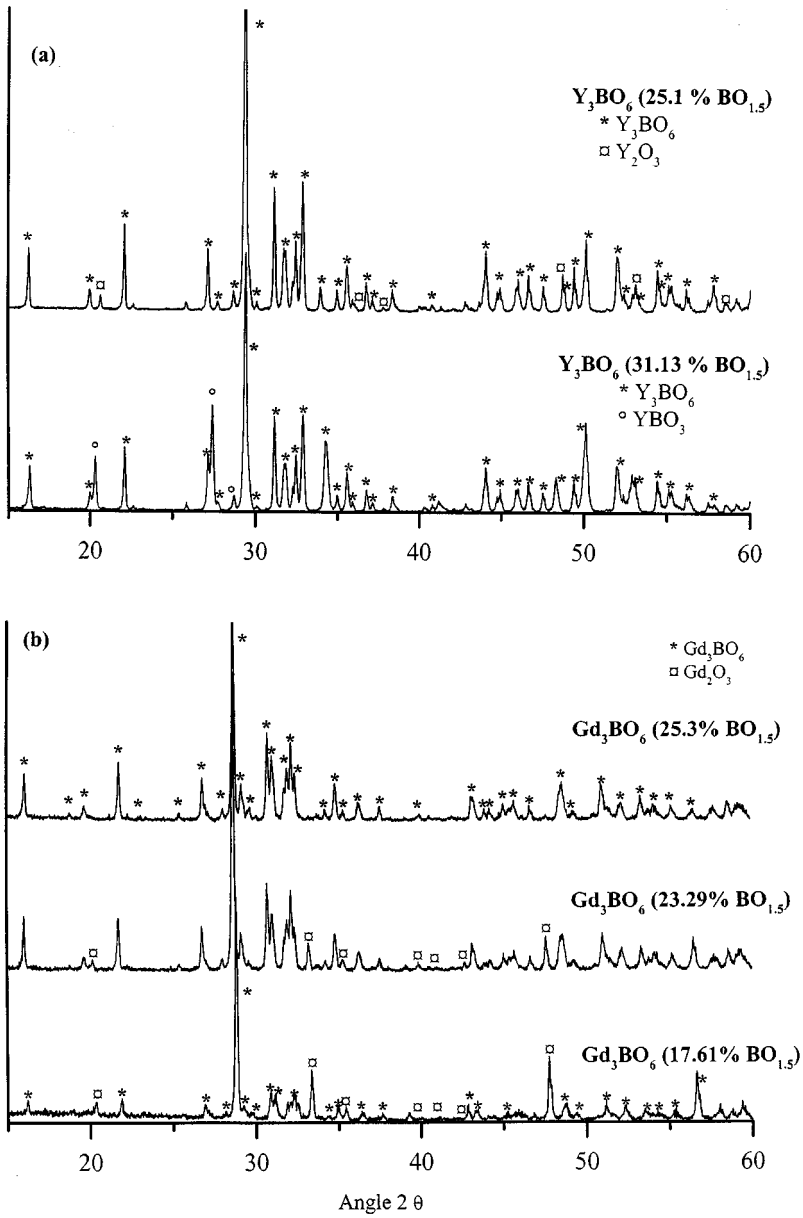

FIG. 7. X-ray diffraction pattern of Ln_3BO_6. (a) For Ln = Y, at 31.1 and 25.1 mol% of B_2O_3; (b) for Ln = Gd, between 17.6 and 27.2 mol% of B_2O_3.

For borates with Ln_3BO_6 stoichiometry, the first X-ray crystallographic data were given by Leskalä and Niinistö (13) in 1986. The structure was considered as an orderly arrangement of all atoms within the crystal. The sharp characteristics of the diffractograms were interpreted by the authors as due to the absence of rotational disorder of the borate groups. Orthoborate BO_3^{3-} group was considered as the only possible arrangement to satisfy the requirements of crystal symmetry and chemical stoichiometry.

Recently, Lin *et al.* (14, 15) proposed $Ln_{17.33}(BO_3)_4(B_2O_5)O_{16}$ as the composition of previously known Ln_3BO_6 with Ln = Y and Gd. The structure would contain two different kinds of BO_3^{3-} and $B_2O_5^{4-}$, with a B–O–B angle about 150°.

We have reinvestigated the stoichiometry of Ln_3BO_6 for Ln = Y and Gd. As it is difficult to obtain pure compounds, two yttrium samples were prepared for 25.1 and 31.1 mol% B_2O_3. The comparison of the X-ray diffraction patterns (Fig. 7a) shows that for 25.1 mol% B_2O_3, Y_2O_3 is present as weak impurity and for 31.1 mol% B_2O_3, the sample is two-phased YBO_3 and Y_3BO_6. The stoichiometry of Ln_3BO_6 is also confirmed for Ln = Gd as is shown in Fig. 7b, where X-ray diffraction patterns for 25.3 mol% of B_2O_3 can be indexed as Gd_3BO_6 using the Leskalä and Niinistö data (13). When B_2O_3 content decreases below 25 mol%, the main characteristic lines of Gd_2O_3 appear. Our results confirm the stoichiometry Ln_3BO_6 for Ln = Gd and Y. A small homogeneity range has not to be excluded, but it is not realistic that it was extended up to 31.6 mol% of B_2O_3.

Boron and yttrium environments have been investigated by MAS MNR and, as it was done previously, the structural environments of boron and gadolinium atoms in Gd_3BO_6 were determined through the analog compound Y_3BO_6.

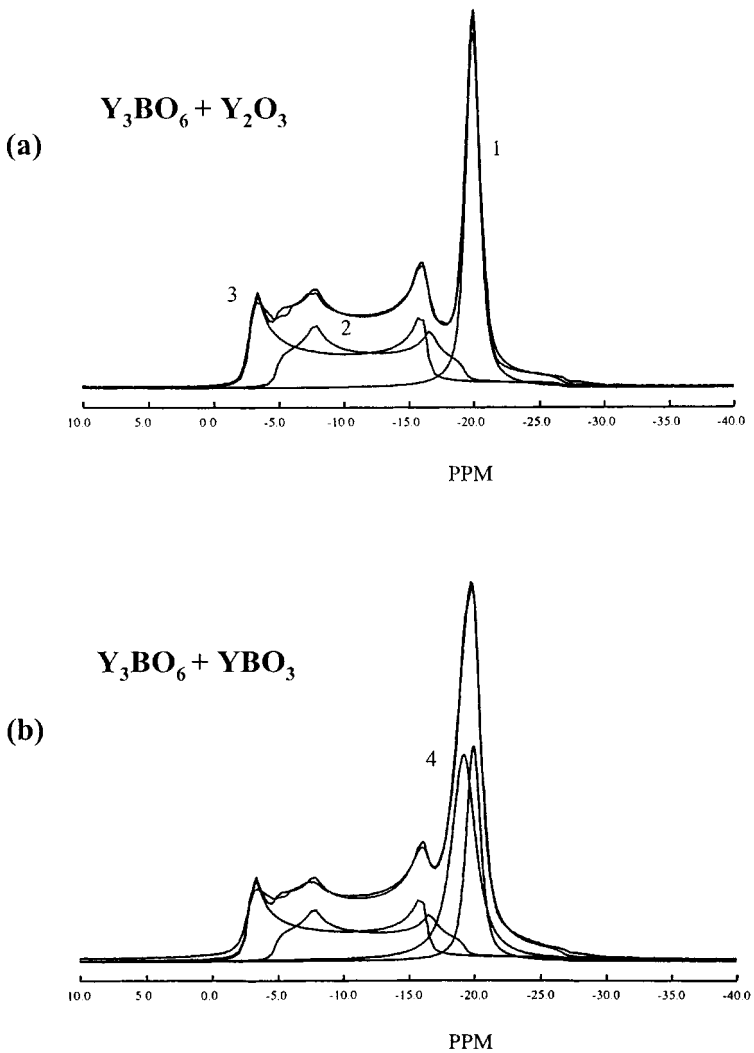

FIG. 8. ^{11}B spectra of Y_3BO_6. (a) For Y_3BO_6 containing Y_2O_3; (b) For Y_3BO_6 containing YBO_3.

^{11}B. Figure 8 shows that two different threefold and one fourfold coordinated boron are present in a 1:1:1 ratio. One B^{III} site, with a quadrupolar asymmetric parameter $\eta_Q = 0.02$, is in agreement with a planar triangulary BO_3^{3-} group; the second B^{III} site would be distorted ($\eta_Q = 0.22$). For sample containing YBO_3, the two B^{IV} sites (one for Y_3BO_6 and one for YBO_3) are clearly distinguished by simulation.

^{89}Y. Figure 6 shows the result of simulation concerning the spectra of sample containing Y_3BO_6 and YBO_3. The signal relative to ^{89}Y in orthoborate differs clearly from those relative to Y_3BO_6. Simulation permits the separation 15 of different sites occupied by yttrium atoms with relative population of approximatively $(1)_{10}$:$(2)_2$:4:5:9.

CONCLUSIONS

In the Gd_2O_3–B_2O_3 binary system, three solid phases with respective stoichiometry Gd_3BO_6, $GdBO_3$, and $Gd(BO_2)_3$ have been evidenced. Orthoborate melts congruently, and the two others decompose before melting.

$GdBO_3$ presents a very narrow existing field and at about 900°C a structural transition occurs induced by a progressive change of the boron environment. At room temperature, MAS NMR experiments show only fourfold boron atoms. When temperature increases the change of the chemical shift of the boron signal traduces formation of threefold boron with fast exchange between B^{IV} and B^{III}. The existence of two kinds of yttrium atoms is confirmed.

For Ln = Y and Gd, the stoichiometry of Ln_3BO_6 was confirmed and disagrees with the results of Lin *et al.* (14, 15). The boron environment in Gd_3BO_6 is constituted by two kinds of B^{III} and one B^{IV} in equivalent proportion. Simulation of ^{89}Y spectra makes it possible to distinguish 15 different Y sites. These results are not yet interpreted.

REFERENCES

1. S. R. Chinn and H. Y. P. Hong, *Opt. Commun.* **18,** 87 (1976).
2. E. M. Levin, R. S. Roth, and J. B. Martin, *Am. Mineral.* **46,** 1030 (1961).
3. S. F. Bartram, "Rare-Earth Research," Vol. II, p. 165. Gordon and Breach, New York, 1965.
4. G. D. Abdullaev, Kh. S. Mamedov, and G. D. Dzhafarov, *Sov. Phys. Crystallogr.* **20**(2), 161 (1975).
5. J. H. Denning and S. D. Ross, *Spectrochem. Acta* **23A,** 1775 (1972).
6. F. Bartram and E. J. Felten, "Rare Earth Research," Vol. 2, p. 330. Gordon and Breach, New York, 1962.
7. R. E. Newnham, M. J. Redman, and R. P. Santoro, *J. Am. Ceram. Soc.* **46**(6), 253 (1963).
8. C. E. Weir and E. R. Lippincott, *J. Res. Nat. Bur. Stands* **65A,** 173 (1961).
9. C. E. Weir and R. A. Schroeder, *J. Res. Nat. Bur. Stands* **68A,** 465 (1964).
10. J. P. Laperches and P. Tarte, *Spectrochem. Acta* **22,** 1201 (1966).
11. W. F. Bradley, D. L. Graf, and R. S. Roth, *Acta Crystallogr.* **20,** 284 (1966).
12. G. Chadeyron, M. El-Ghozzi, R. Mahiou, A. Arbus, and J. C. Cousseins, *J. Solid State Chem.* **125,** 261 (1997).
13. M. Leskalä and L. Niinistö, *in* "Handbook on Physics and Chemistry of Rare-Earth," (K. A. Gschneidner, Jr., and L. Eyring, Ed.), p. 203. Elsevier Science, Amsterdam, 1986.
14. J. H. Lin, S. Zhou, L. Q. Yang, G. Q. Yao, and M. Z. Su, *J. Solid State Chem.* **134,** 158 (1997).
15. J. H. Lin, L. P. You, G. X. Lu, L. Q. Yang, and M. Z. Su, *J. Mater. Chem.* **8**(4), 1051 (1998).